Astron. Astrophys. 338, 122–126 (1998)

ASTRONOMY
AND
ASTROPHYSICS

HV Tauri C – Herbig-Haro flow or stellar companion with strong forbidden emission lines?

J. Woitas and Ch. Leinert

Max-Planck-Institut für Astronomie, Königstuhl 17, D-69117 Heidelberg, Germany

Received 10 June 1998 / Accepted 7 July 1998

Abstract. We present new near- and mid-infrared photometry of the infrared source near HV Tau that was proposed as a Herbig-Haro object by Magazzù & Martin (1994). We draw a different conclusion, namely that this object is a T Tauri star with strong forbidden emission lines as had been suggested originally. The presence of a Herbig-Haro flow in the vicinity of a weak-lined T Tauri star like HV Tau would have imposed a problem on models of T Tauri stars and their environment. With the reinstatement of the companion to HV Tau as a T Tauri star this problem disappears.

Key words: stars: pre-main sequence – stars: binaries: general – stars: individual: HV Tau C

1. Introduction

T Tauri stars are divided into classical T Tauri stars (CTTS) and weak-lined T Tauri stars (WTTS) using the equivalent width of the $H\alpha$ emission line as criterion (e. g. Walter et al. 1986). CTTS – usually taken as those having $W(H\alpha) \geq 10Å$ – show IR- and UV-excesses indicative of circumstellar accretion disks. There is a link between accretion and outflow phenomena in young stellar objects: Forbidden line emission (arising in the outflow) and optical veiling (produced by accretion onto the YSO) are only found in objects that exhibit an IR color excess (Königl 1994). Further, the interaction of the stellar winds of young stars with their environment causes phenomena like molecular flows, stellar jets and Herbig-Haro objects (Appenzeller & Mundt 1989). In contrast, WTTS have much less prominent disk emission and show lesser signs of activity.Therefore it was a surprise that Magazzù & Martin (1994, hereafter MM) claimed to have found a Herbig-Haro object driven by the WTTS HV Tau, despite the fact that the spectrum of this presumed HH object showed a rather prominent continuum and its images were typical of a stellar object (i. e. with circular intensity contours).

HV Tau was presented as a triple system by Simon et al. (1992). Using lunar occultation observations at $2.2\,\mu m$ they detected the companion HV Tau B with a projected separation of (35 ± 2) mas at a position angle of $273° \pm 13°$ relative to HV Tau A. HV Tau B is less bright than HV Tau A by a factor 0.58 ± 0.05 at this wavelength. The presence of HV Tau B has been confirmed by measurements conducted with the HST Fine Guidance Sensors (Simon et al. 1996). Since the observational techniques used in our study cannot resolve this close pair, we will henceforth call the main component HV Tau AB and its properties will refer to the sum of these two stars. The second companion HV Tau C has been found by subsequent K-band imaging of the source at a projected separation of $4''.0$ and a position angle of 45° (Simon et al. 1992). MM have proposed that HV Tau C is in fact no stellar companion but identical with the Herbig-Haro object mentioned above.

Send offprint requests to: woitas@mpia-hd.mpg.de

2. Observations and data reduction

Images of the HV Tau system in the spectral bands J, H, K and L were obtained on 25 August 1996 at the United Kingdom Infrared Telescope (UKIRT), using the infrared camera IRCAM3. A series of five frames was taken for each spectral band, with the star moving on the array from one image to another. For reduction first a dark is subtracted from the images, then a sky frame is constructed by median combining the images, and finally this sky is subtracted from the dark subtracted frames.

The HV Tau system was again observed at UKIRT on 30 August 1996. N-band data were taken with the *M*id-infrared *A*rray e*X*pandable (MAX) camera. The telescope was chopped N-S at a rate of $2.2\,Hz$. Images obtained at one final position of this chopping are subtracted from the images taken at the other final position. In this way bias, dark current and thermal background are removed. These sky subtracted images were bad pixel corrected.

On 14 February 1998 additional images of HV Tau in the infrared emission lines $Br\gamma$ and H_2 (S 1-0) were taken at the Calar Alto $3.5\,m$ telescope using the *Omega Cass* camera. The images were sky subtracted,flatfielded and bad pixel corrected. Then the brightest pixel of each frame was centered and all frames taken in one filter were coadded to obtain the final images (Fig. 1a,b).

On the reduced images aperture photometry is done using the IRAF APPHOT package. The components are distinctly separated in all filters, but the point spread function of HV Tau AB is still above zero at the distance of component C. To correct for this, we have measured the sky background for HV Tau C

Table 1. Relative positions of main component and companion from previous observations compared to the results derived from our measurements

Author	Projected separation	Position angle	Method	Date of observation
Simon et al. (1992)	$4''.00 \pm 0''.40$	$45° \pm 5°$	imaging: K	Oct 1990
Magazzù & Martin (1994)	$4''.03$	$43°.2$	imaging: Hα, S II	Jan 1991
This paper	$3''.98 \pm 0''.03$	$43°.5 \pm 0°.4$	imaging: JHKL	26 Aug 1996
This paper	$3''.99 \pm 0''.31$	$44° \pm 5°$	imaging: N	30 Aug 1996
This paper	$4''.03 \pm 0''.24$	$45°.8 \pm 2°.0$	imaging: H_2, Brγ	14 Feb 1998

Table 2. Photometry of the HV Tau system

Filter	HV Tau AB	HV Tau C	Δ mag
J	9.12 ± 0.12	13.34 ± 0.12	4.22
H	8.25 ± 0.09	12.53 ± 0.09	4.28
K	7.92 ± 0.06	12.14 ± 0.07	4.22
L	7.56 ± 0.09	≥ 9.27	≥ 1.71
N	6.32 ± 0.29	7.31 ± 0.32	0.99
Brγ			4.86
H_2			4.47

Table 3. Flux of HV Tau C at different wavelengths

Wavelength μm	Magnitude	Flux $10^{-19}\,\mathrm{Wcm^{-2}sr^{-1}\mu m^{-1}}$
0.55	17.25	4.53
0.64	15.81	10.7
0.79	14.93	13.1
1.25	13.34 ± 0.12	13.9 ± 1.5
1.65	12.53 ± 0.09	10.9 ± 0.9
2.2	12.14 ± 0.07	5.49 ± 0.35
10.6	7.31 ± 0.32	1.03 ± 0.33

in an aperture as large as that used for the star and in the same distance from HV Tau AB.

To quantify the separation of HV Tau C we need plate scale and orientation [1] for the various observations. For the IRCAM3 camera an array orientation of $1.8° \pm 0.4°$ and a pixel scale of $(0''.281 \pm 0''.002)/\mathrm{pixel}$ is given in the manual. We have used a N-band image of XZ Tau and HL Tau which are separated by 23''.7 to derive pixel scale and array orientation for our MAX measurements. Estimating a positional error of 1 pixel, we obtain $(0''.266 \pm 0''.003)/\mathrm{pixel}$ respectively $1.1° \pm 0.7°$. For the *Omega Cass* observations we can get the array orientation from a trailed image (without tracking) and the pixel scale from the separation of 101''.3 of HV Tau AB from the nearby star DO Tau which is visible on some of the images. We obtain $22.5° \pm 2.0°$ and $(0''.120 \pm 0''.005)/\mathrm{pixel}$. The images shown in Fig. 1 of MM have a pixel scale of $0''.303/\mathrm{pixel}$ and an orientation of $-90°$ (A. Magazzù, private communication). Table 1 lists the resultant position angles and separations [2] of HV Tau C with respect to HV Tau AB for the above observations. We add the values given in Simon et al. (1992). All relative positions are consistent within their uncertainties, so we can be confident that the object has shown no measurable proper motion within seven and a half years.

3. Results

Fig. 1a–e shows images of the HV Tau system in the NIR emission lines Brγ and H_2 and in the broad-band filters J, H and K. From this we can derive the relative flux of HV Tau C with respect to HV Tau AB given in Table 2.

In Table 2 also the results of our JHKLN-photometry are shown. HV Tau C was not detectable in the L-band (the upper limit shown is 3σ above background level), but definitely seen at $10\,\mu$m. We adopt an interstellar extinction $A_V = 1.91$ (Kenyon & Hartmann 1995) and the reddening law of Rieke & Lebofsky (1985) to derive dereddened colors $J - H = 0.60$, $H - K = 0.265$ and $K - N = 4.72$.

The JHKLN magnitudes from Table 2 and the VRI values given in MM were converted into fluxes using the conversion factors given by Leinert et al. (1998). The result is shown in Table 3. We adopt the K-band brightness ratio $I_B/I_A = 0.58 \pm 0.05$ for all spectral bands and in this way estimate fluxes separately for HV Tau A and B, too. So we can plot the dereddened spectral energy distributions for the three components of the HV Tau system (Fig. 2). The SEDs of HV Tau A and B can be reasonably well connected with blackbody curves for $\mathrm{T} = 2800\,\mathrm{K}$, except for small excesses in the N-band. For HV Tau C a blackbody of $\mathrm{T} = 3700\,\mathrm{K}$ suits well from V to K, but there is strong excess emission in the N-band.

4. Discussion

There are several reasons why HV Tau C should be considered as a stellar object:

– The companion appears to be circular in all of our images and particularly in the images taken in the filters Hα, [S II] and 684 nm continuum by MM (Fig. 1 therein). No elongated structures or shockfronts are visible as one might expect in the case of a Herbig-Haro object.
– HV Tau C does not show significant motion relative to HV Tau AB (Table 1). Consider a Herbig-Haro object

[1] Orientation here means the angle between the northern direction on the sky and the top direction on the array, measured on the array from top to left.

[2] The separation of 5'' that is given by MM is erroneous. This has been confirmed by A. Magazzù.

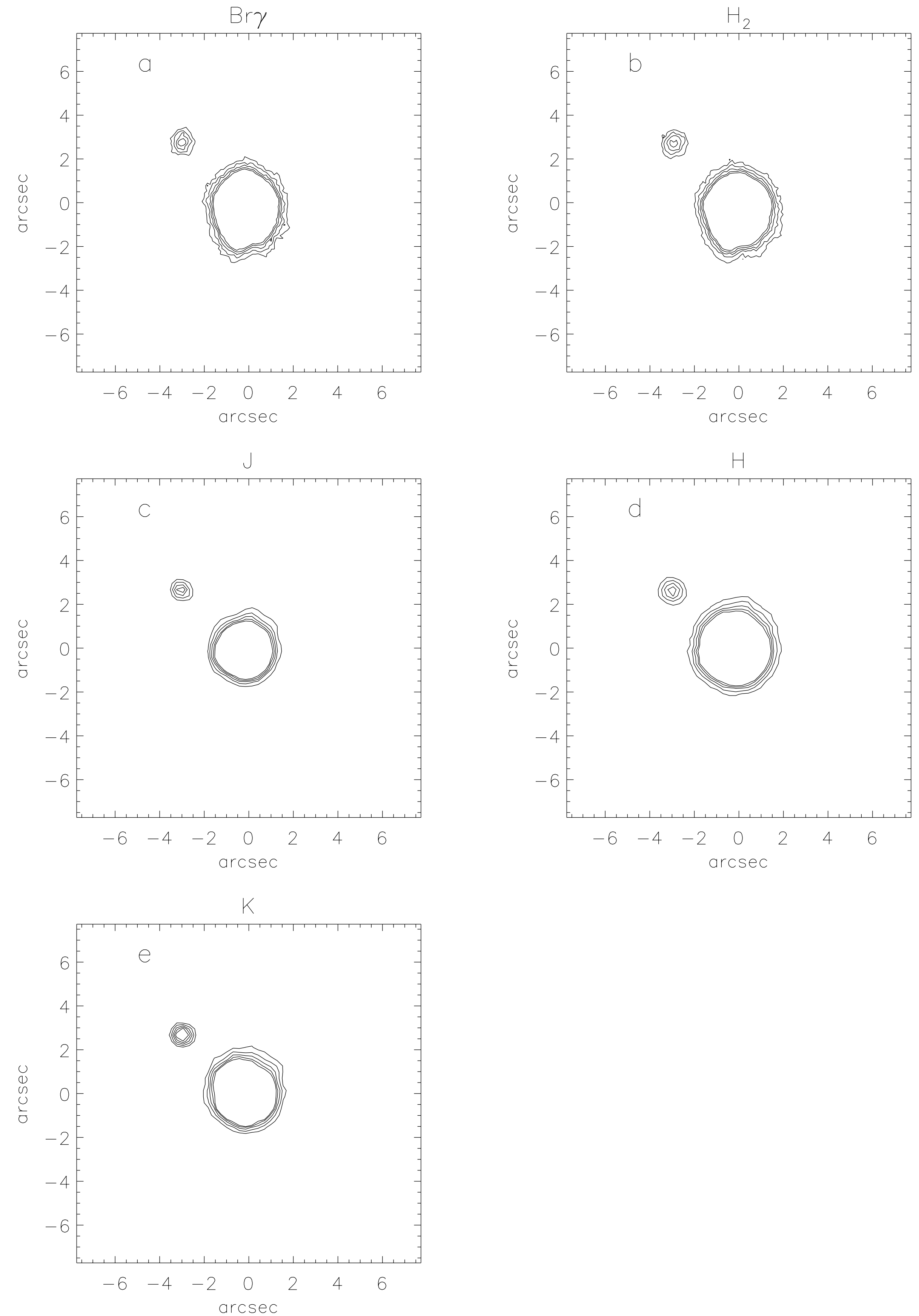

Fig. 1a–e. Images of the HV Tau system in the filters Brγ, H_2 (S 1-0), J, H and K. North is at the top in all of the images. The contour levels are 60, 85, 110, 135 and 160 counts.

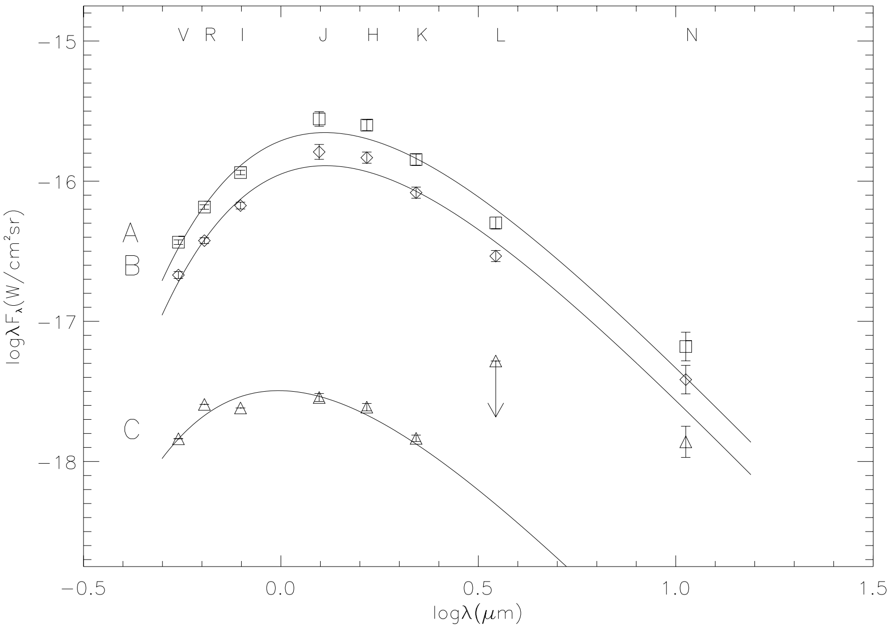

Fig. 2. Spectral energy distributions of HV Tau A, B and C, dereddened with $A_{\mathrm{V}} = 1.91$, fit with blackbodies of $2800\,\mathrm{K}$ (components A and B) and $3700\,\mathrm{K}$ (component C). The spectral indices for different stars are plotted as squares (A), diamonds (B) and triangles (C). For the sake of clearness the curves for HV Tau A and B were shifted upward by 0.5.

moving away from its driving source with a velocity of $v_{\mathrm{r}} \approx 100\,\mathrm{km/s}$ – which is on the low side for a HH object. This object would have moved about $1''$ relative to the main component within eight years contrary to the observations. On the other hand, measurable orbital motion has not to be expected for a separation of $4\overset{''}{.}0$ corresponding to $600\,\mathrm{AU}$. So the relative astrometry also suggests that HV Tau C is a stellar companion.

– The spectrum of HV Tau C shows strong continuum emission (MM, Fig. 2 therein). This would be very unusual for a Herbig-Haro object, but is the typical signature of a star.
– HV Tau C does not show a prominent brightness in the NIR emission lines Brγ and H_2 (Fig. 1a,b). In fact the brightness ratio of the companion relative to the main component is even lower in Brγ and H_2 than in the broadband NIR-filters J, H and K (Table 2).
– The spectral energy distribution of HV Tau C is typical for a system consisting of a star and a circumstellar disk. From 0.55 to 2.2 μm the SED can reasonably well be fit with a blackbody, suggesting that in these wavelengths the source of radiation is a stellar photosphere. At $10.6\,\mu\mathrm{m}$, however, there is a distinct excess that can be explained by reprocessed starlight from a circumstellar disk and by emission due to active accretion (e. g. Beckwith et al. 1990). The presence of a circumstellar disk is also in line with the equivalent width of $\mathrm{W(H}\alpha) \approx 15\text{Å}$ from Fig. 4 in MM, which classifies HV Tau C as a classical T Tauri star.

On the other hand, we do not fully accept the arguments given in support of a Herbig-Haro nature for HV Tau C:
The first argument of MM for HV Tau C being a Herbig-Haro object was based on a comparison of the relative emission line intensities found in HV Tau C to values for the high excitation Herbig-Haro object HH 2H published by Schwartz (1983). However, this comparision is not matching well for all of the emission lines: In the [N II] lines at $654.7\,\mathrm{nm}$ and $658.3\,\mathrm{nm}$ respectively and for the combined [O II],[Ca II] line at $732.8\,\mathrm{nm}$ there are discrepancies of about a factor two. Certainly the intensities of the [O I] lines at $630.0\,\mathrm{nm}$ and $636.4\,\mathrm{nm}$ and the [S II] lines at $671\,\mathrm{nm}$ and $673.1\,\mathrm{nm}$ measured relative to the Hα intensity are very much the same for HH 2H and HV Tau C, but these line ratios differ largely from one HH object to another as Table 4 shows.

Forbidden emission lines are common in T Tauri stars as can be seen from Hartigan et al. (1995, Table 3 therein). The intensity ratio [O I]/[S II] for the T Tauri stars lies between one and five and, hence, in the same order of magnitude as that for HV Tau C. Moreover, Mundt et al. (1990) have pointed out that this line ratio has almost the same spatial distribution for the T Tauri star XZ Tau and the Herbig-Haro object HH 30. So it is not possible to classify HV Tau C as a HH object using the intensity ratio [O I]/[S II] as a criterion.

Another argument presented by MM was the existence of two velocity components in the emission lines that are visible in their high resolution spectra (MM, Fig. 3 therein). They interpret this as signature of a radiative bow shock. Given the fact that no shock structures are visible in the images that have been taken from HV Tau C (Fig. 1a–e and Fig. 1 in MM), we think that it is more resonable to explain this feature as the result of a bipolar outflow emanating from the *star* HV Tau C. It has already been mentioned that the mid-infrared excess emission and the equivalent width $\mathrm{W(H}\alpha) \approx 15\text{Å}$ suggest that HV Tau C is an active T Tauri star with an accretion disk and a bipolar outflow emanating perpendicular to this disk. Assuming that we are looking onto this disk nearly edge-on ($i_{\mathrm{disk}} \approx 85°$) and estimating a typical outflow velocity of about $300\,\mathrm{km/s}$ we derive a Doppler shift of $\pm 26\,\mathrm{km/s}$ for the two outflow components that would fit well with the structure of the emission lines given by MM (Fig. 3 therein).

Table 4. Line intensities relative to $\mathrm{I(H\alpha)} = 100$ for HV Tau C and some Herbig-Haro objects. The values for HH 2H and HH 47 are taken from Schwartz (1983), those for HH 34 and HH 111 from Bacciotti et al. (1995)

Object	[O I]λ6300	[O I]λ6364	[S II]λ6716	[S II]λ6731
HV Tau C	42	15	13	29
HH 2H	40.3	14.6	12.6	24.8
HH 34	285	93	249	281
HH 47	69.1	21.9	105.3	101.7
HH 111	135	34	145	173

The last argument of MM for HV Tau C being a Herbig-Haro object was that the colors V-I and V-K are bluer than those derived for HV Tau AB. The SEDs (Fig. 2) indeed suggest that HV Tau C is of higher temperature and, hence, bluer than the other components of the system, but the resultant temperature $T_{\mathrm{eff}} = 3700\,\mathrm{K}$ matching with a spectral type of M0.5 (Bessell 1991) is still in a range common for T Tauri stars as well as the infrared colors J-H, H-K and K-N (Kenyon & Hartmann 1995, Table 2 therein). Additional extinction in an almost edge on circumstellar disk and scattering in the bipolar lobes could combine to make HV Tau C appear both fainter and bluer than the main component.

It should be mentioned that the optical spectrum of HV Tau C (Fig. 2 in MM) does not show prominent molecular absorption lines despite the fact that its colors are those of an M star. If HV Tau C indeed is intrinsically fainter and cooler than the main component, this would imply strong veiling by disk accretion. In the case that component C is of earlier spectral type, as just discussed, this is a lesser problem.

As result of this discussion we propose that HV Tau C is an active T Tauri star with strong forbidden emission lines.

Acknowledgements. We thank Tom Herbst, Paul Kalas and Massimo Robberto very much for doing the observations and their help in reducing the data. The authors appreciate fruitful discussions with Reinhard Mundt and Michael Meyer. Björn Seidel has helped in producing the figures. This research has made use of the SIMBAD database,operated at CDS, France.

References

Appenzeller, I., Mundt, R.: 1989, A&AR 1, 291
Bacciotti, F., Chiuderi, C., Oliva, E.: 1995, A&A, 296, 185
Beckwith, S.V.W., Sargent, A.I., Chini, R.S., Güsten, R.: 1990, AJ, 99, 924
Bessell, M.S.: 1991, AJ 101, 662
Hartigan, P., Edwards, S., Ghandour, L.: 1995, ApJ, 452, 736
Kenyon, S.J., Hartmann, L: 1995, ApJS, 101, 117
Königl, A.: 1994, Theory of Outflows. In: Disks and Outflows Around Young Stars, Beckwith, S., Staude, J., Quetz, A., Natta, A. (eds.), Lecture Notes in Physics, vol. 465, 282
Leinert, Ch., Bowyer, S., Haikala, L.K., Hanner, M.S., Hauser, M.G., Levasseur-Regourd, A.-Ch., Mann, I., Mattila, K., Reach, W.T., Schlosser, W.T., Staude, H.-J., Toller, G.N., Weiland, J.L., Weinberg, J.L., Witt, A.N.: 1998, A&AS 127, 1
Magazzù, A., Martin, E.L.: 1994, A&A 287, 571 (MM)
Mundt, R., Ray, T.P., Bührke, T., Raga, A.C., Solf, J.: 1990, A&A, 232, 37
Rieke, G.H., Lebofsky, M.J.: 1985, ApJ, 288, 618
Schwartz, R.D. : 1983, ARA&A 21, 209
Simon, M., Chen, W.P., Howell, R.R., Benson, J.A., Slowik, D.: 1992, ApJ 384, 212
Simon, M., Holfeltz, S.T., Taff, L.G.: 1996, AJ, 469, 890
Walter, F.M., Vrba, F.J., Mathieu, R.D., Brown, A., Myers, P.C.: 1986, ApJ 306, 573